JOURNAL OF Applied Polymer SCIENCE

Effect of Bamboo Charcoal Powder on the Curing Characteristics, Mechanical Properties, and Thermal Properties of Styrene-Butadiene Rubber with Bamboo Charcoal Powder

Xianghai Meng,[1] Yihe Zhang,[1,2] Jinbo Lu,[1] Zhilei Zhang,[1] Leipeng Liu,[1] Paul K. Chu[2]

[1]National Laboratory of Mineral Materials, School of Materials Science and Technology, China University of Geosciences, Beijing 100083, China

[2]Department of Physics and Materials Science, City University of Hong Kong, Tat Chee Avenue, Kowloon, Hong Kong, China

Correspondence to: Y. Zhang (E-mail: zyh@cugb.edu.cn)

ABSTRACT: Compounds of styrene–butadiene rubber (SBR) filled with bamboo charcoal powders (BCPs) were prepared with a laboratory-sized two-roll mill. The effects of the BCP loading on the curing characteristics and mechanical and thermal properties were investigated. The results indicate that the addition of BCP resulted in a longer curing time and a higher Mooney viscosity in the SBR materials. The incorporation of BCP into SBR improved the mechanical properties and dynamic properties. Furthermore, the mechanical properties of the vulcanizates after thermal aging were also studied, and the experimental results indicate that most of the mechanical properties improved after thermal aging. The overall results indicate that BCP could be used as a cheaper filler for SBR materials. © 2013 Wiley Periodicals, Inc. J. Appl. Polym. Sci. 000: 000–000, 2013

KEYWORDS: composites; manufacturing; mechanical properties; rubber; thermal properties

Received 8 December 2012; accepted 8 May 2013; Published online
DOI: 10.1002/app.39522

INTRODUCTION

Styrene–butadiene rubber (SBR) is amorphous and has better processability, heat aging, and abrasion resistance but is inferior in terms of physicomechanical characteristics with reinforcing fillers. Thus, it has been appropriate for many applications,[1] such as the production of tires and different rubbers goods.[2] Carbon black is unquestionably the most widely used reinforcing filler in the rubber industry. However, because of its dependence on petroleum feedstock (for synthesis), the instability of the price of petroleum has resulted in increasing interest in other reinforcing fillers.[3] Reinforcement with fillers from renewable resources into polymeric materials has become a major interest in recent years. According to reports, lots of fillers have been used to take the place of the commonly used carbon black; these include silicates,[4,5] montmorillonite,[6–9] and reinforcing fillers from renewable resources such as rice husks,[10–15] starch,[16–20] chitosan,[21] oil palms,[22–24] chitin,[25] and cuttlebones.[26–28]

Bamboo is an abundant and inexpensive natural resource. It can be carbonized in a furnace at high temperature in the absence of oxygen to produce bamboo charcoal. Bamboo charcoal is an environmentally friendly, low-cost (ca. $421–571/ton), and renewable bioresource in China.[29] However, its utilization has not been fully explored. Bamboo charcoal is characterized by a high density, a porous structure, and a huge specific surface area.[30] According to the literature, bamboo charcoal with an excellent adsorption capacity was used as a potential adsorbent for the removal of various kinds of pollutants, including nitrate–nitrogen,[31] dibenzothiophene,[32,33] phenol,[34–36] heavy metals,[29,37–40] ammonia,[41] and dye.[42–45] Because of the high carbon content,[46] bamboo charcoal may provide an alternative option and to partly replace conventional fillers in the rubber industry. Therefore, as a renewable and low-cost filler, bamboo charcoal and its uses may deserve more attention.

In this article, bamboo charcoal powder (BCP) was used as a new type of filler in SBR. The properties, including the curing characteristics and mechanical and thermal properties, of the composites were characterized in detail. One of the most important requirements for BCP to be successfully used as a filler is its good interaction with rubber at a reasonable loading level. Therefore, the effects of BCP on the curing characteristics and mechanical and thermal properties of SBR filled with BCP were examined.

EXPERIMENTAL

Materials

SBR latex with a solid content of 17.46 wt % and other compounding ingredients, including zinc oxide, stearic acid, *N-tert*-butyl-2-benzothiazole sulfonamide (TBBS), and sulfur,

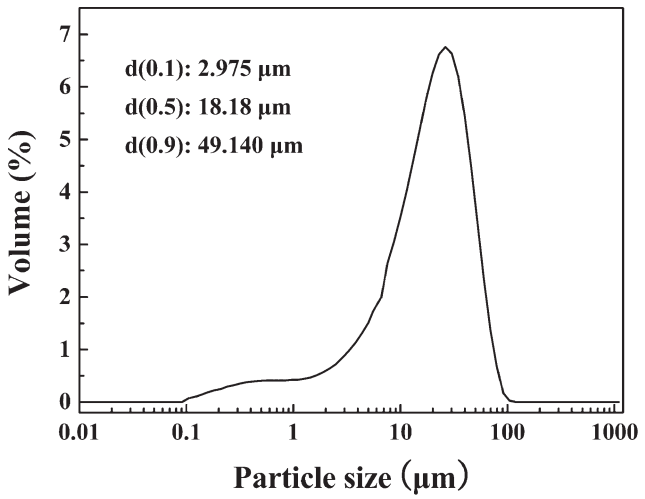

Figure 1. Particle size of BCP. The numbers following "d" in parentheses indicates the volume fraction. For example, "d(0.1):2.975" indicate that the volume fraction is 10% whose particle size is below 2.975 μm.

were all purchased from Qilu Petrochemical Co. (Shandong, China). BCP with an average particle size of 18.18 μm (shown in Figure 1) was obtained from International Centre for Bamboo and Rattan (Beijing, China). The flocculating agent was purchased from Fengquan Chemical Co. (Shandong, China). Sodium chloride, sulfuric acid, and sodium hydroxide was purchased from Chemical Reagent Beijing Co., Ltd. Commercial-grade carbon black (N330) with an average particle size of 17.5 μm was used in this study.

Mixing and Curing Assessment

BCP was continuously agitated in the SBR latex; then, the mixture was treated by an ultrasonic processing technique for 30 min. Sodium chloride (10 g) and the flocculating agent (6 mL) were dissolved in distilled water (350 mL), and the pH of solution was determined at 3–3.5 through the addition of sulfuric acid. Then, the solution was heated to 55–60°C, and we added this to the mixture of BCP and SBR latex. The rubber-incorporated BCP was leached from the suspension, and aqueous sodium hydroxide was used to neutralize the acid solution. When the rubber-incorporated BCP was dried at 60°C for 24 h, the compounding of SBR with BCP and the other ingredients, as shown in Table I, were performed with a laboratory-sized two-roll mill [model X(S)K-160]. The compounded rubber was left for 24 h before vulcanization. The optimum curing characteristics of the compounds were determined with a rotorless rubber curometer (RC2000E) at 150°C.

Table I. Composition of the SBR Compounds

Material	Compound (phr)[a]
SBR rubber	100
Zinc oxide	3
Stearic acid	1
TBBS	1
Sulfur	1.75
BCP	0, 10, 20, 30, 40, 50, 60

The cure rate index (CRI) was measured according to ISO 6502[8]. The following formula was used to determine CRI in this study:

$$\mathrm{CRI} = 100/(T_{90} - t_{s2}) \quad (1)$$

where t_{s2} is the scorch time and T_{90} is the curing time. The changes in the torque with filler loading was used to characterize the filler–matrix interaction or reinforcement. The reinforcement factor (α_f) was calculated from the rheographs[47,48] and is given by the following equation:

$$\alpha_f = \left[\Delta L_{\max\,(\mathrm{filled})} - \Delta L_{\max\,(\mathrm{controlled})}\right] / \Delta L_{\max\,(\mathrm{controlled})} \quad (2)$$

where $\Delta L_{\max(\mathrm{filled})}$ and $\Delta L_{\max(\mathrm{controlled})}$ are the changes in the maximum torque during vulcanization for the filled and controlled compounds, respectively.

The compounds were compression-molded at 150 ± 1°C according to the respective T_{90} values with a laboratory hydraulic press (QLB-25D/Q), and the pressure was controlled at 15–20 MPa. The Mooney viscosity (ML_{1+4} at 100°C) was determined with a Mooney viscometer (MV200E).

Measurement of the Tensile Properties

The effect of the thermal aging on the properties of the SBR filled with BCP was studied according to the standard method ASTM D 573-99 (1999). The vulcanizates were aged at an oven temperature of 70°C for 96 h and then left at room temperature for 16 h before testing. The mechanical properties of the vulcanizates before and after thermal aging were then evaluated. Dumbbell-shaped test pieces were cut from molded sheets previously conditioned for 24 h at room temperature. Tensile tests were performed with an electronic versatile tester (CMT 4304) at a crosshead speed of 500 mm/min. The tensile strength and elongation at break were obtained from the tests. Five dumbbell-shaped samples were tested for reduplication.

Measurement of the Dynamic Properties

The dynamic mechanical analysis (DMA) spectra of the samples were obtained with a Seiko SII advanced dynamic mechanical spectrometer (model DMS6100). Specimens with a size of 40 × 8 × 1 mm^3 were analyzed in tensile mode at a constant frequency of 10 Hz and a temperature range from −80 to 100°C at a heating rate of 4°C/min in a nitrogen atmosphere. The temperature corresponding to the peak in the dynamic loss tangent (tan δ) versus temperature plot was taken as the glass-transition temperature (T_g).

Measurement of the Thermal Properties

Thermogravimetry (TG) was carried out in a thermogravimetric analyzer (Netzsch TG-209C) over a temperature range from room temperature to 550°C at a heating rate of 10°C/min. Nitrogen was used as a purging gas during the process of measurement.

Scanning Electron Microscopy (SEM) Observation of the Fractured Surfaces

Examination of the fracture surface was carried out with a scanning electron microscope (model Hitachi S-4800). All of the surfaces were examined after sputter coating with gold to prevent electrostatic charging and poor image resolution.

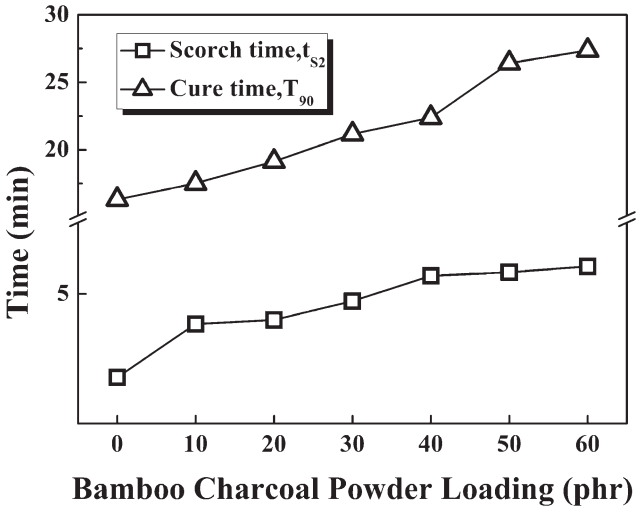

Figure 2. Effect of the BCP loading on the t_{s2} and T_{90} values of the rubber compounds.

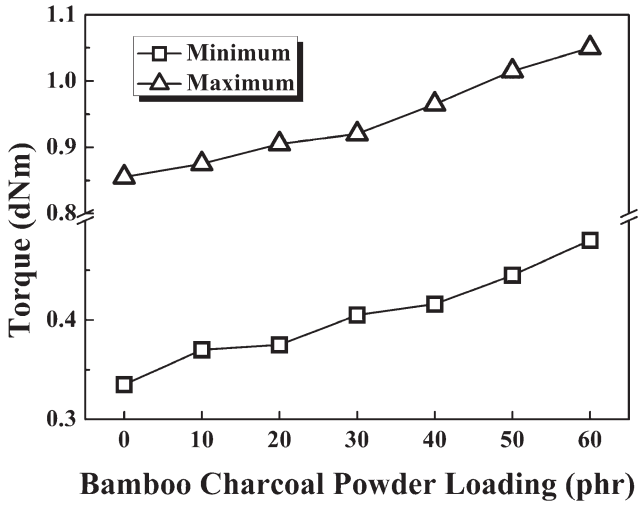

Figure 4. Effect of the BCP loading on the torque of the rubber compounds.

RESULTS AND DISCUSSION

Curing Characteristics

The vulcanization characteristics of the composites are shown in Figures 2–4. We observed that t_{s2} and T_{90} increased along with increasing content of BCP in Figure 2; this indicated that BCP hindered vulcanization. The CRI values (shown in Figure 3)) indicated that the curing rate of the composites decreased as the content of BCP increased; this was due to the delay of the vulcanization process, which resulted from the inclusion of BCP. However, a possible mechanism to explain this phenomenon is still obscure at present.[48]As the curing rate decreased, it was easy to realize safety in the production and prevent the overcuring phenomenon.

α_f described the filler–matrix interaction or reinforcement from the changes in the rheometric torque with filler loading. From the α_f values listed in Figure 3, it was clear that the values of α_f continuously increased with the addition of BCP. This may have been due to the planned choice of the smallest particle sizes to improve the physicomechanical properties. The changes in CRI and α_f may have been due to strong interfacial BCP–rubber interaction.[49]

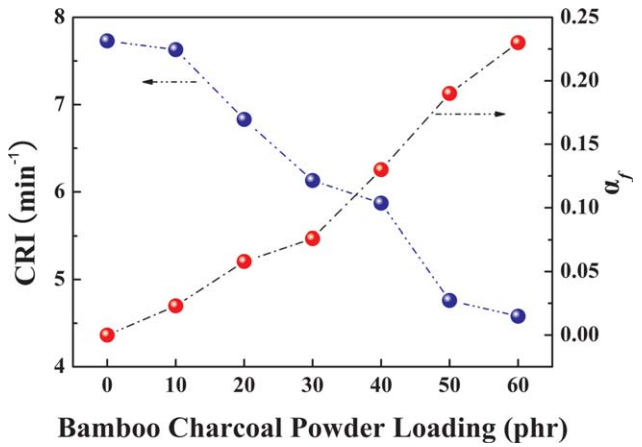

Figure 3. Effect of the BCP loading on the CRI and α_f values of the rubber compounds. [Color figure can be viewed in the online issue, which is available at wileyonlinelibrary.com.]

The torque value of composites is shown in Figure 4. The minimum torque (M_L) values of the composites increased as the BCP loading increased. The increment in the M_L values indicated that the mobility and flexibility of the unvulcanized compounds was reduced with the presence of BCP. As observed, the maximum torque (M_H) values of the composites was similar to the M_L values and exhibited an increasing trend with increasing BCP loading. The mobility and flexibility of the macromolecular chains of rubber were reduced, and the stiffness of the composites was increased with the existence of BCP; this resulted in an increment in the M_H values.[21,50,51] Furthermore, the difference in these values was related to the crosslinking density of the composites. As the value increased, the crosslink densities were expected to increase.[52]

A comparison of the BCP and carbon black in the curing properties is shown in Table II and Figure 5. Compared to BCP, carbon black provided decreases in t_{s2} and T_{90}; this indicated that carbon black accelerated the vulcanization process. Furthermore, the acceleration was also proven from the increase in CRI. The difference in the torque value was obvious, and the variation resulting from BCP was less than that from carbon black. The lesser variation was possibly due to the original channels and porous structure, where the macromolecular chains of rubber could move. The more slight increase in α_f was also due to this reason. The effect of BCP and carbon black on the Mooney viscosity is shown in Figure 5. For BCP and carbon black, the Mooney viscosity substantially increased with increasing filler loading, and SBR filled with BCP had a higher Mooney viscosity. In the mixing state, the large particle size and low interaction (shown from α_f in Figure 3) between the fillers and rubber gave rise to a lower viscosity.[53] The mobility of the rubber's macromolecular chains was reduced with the presence of reinforcing fillers in the rubber matrix. The high values of viscosity for the SBR materials filled with BCP and carbon black indicated that

Table II. Comparison of the Curing and Mechanical Properties of the BCP and Carbon Black

Compound		M_L (dNm)	M_H (dNm)	T_{90} (min)	t_{s2} (min)	CRI (min^{-1})	α_f	T_s (MPa)	E_b (%)
SBR		0.335	0.855	16.33	3.39	7.73	—	2.15 ± 0.15	517 ± 14
Carbon black	10	0.43	1.465	12.19	6.22	16.75	0.71	6.82 ± 1.26	524 ± 16
	20	0.47	1.525	12.34	6.04	15.87	0.78	8.91 ± 1.44	579 ± 19
	30	0.55	1.675	12.32	5.14	13.93	0.96	11.03 ± 1.0	571 ± 35
	40	0.625	1.93	11.49	4.37	14.04	1.26	14.05 ± 0.9	515 ± 27
	50	0.65	1.97	11.32	4.29	14.22	1.3	16.7 ± 0.78	502 ± 23
	60	0.72	2.06	11.02	4.04	14.33	1.41	17.3 ± 0.86	485 ± 12
BCP	10	0.35	0.875	17.52	4.42	7.63	0.023	3.27 ± 0.13	534 ± 9
	20	0.375	0.905	19.14	4.5	6.83	0.058	3.31 ± 0.12	611 ± 13
	30	0.385	0.92	21.16	4.86	6.13	0.076	3.62 ± 0.09	585 ± 9
	40	0.415	0.965	22.39	5.35	5.87	0.13	3.65 ± 0.11	531 ± 7
	50	0.445	1.015	26.42	5.42	4.76	0.19	3.68 ± 0.14	474 ± 12
	60	0.48	1.05	27.36	5.53	4.58	0.23	3.7 ± 0.07	461 ± 8

T_s = tensile strength; E_b = elongation at break.

there was a high restriction to the molecular motion of macromolecules; this was probably caused by the greater interaction between both fillers and SBR.

Tensile Properties

Figures 6–8 shows the effect of the BCP loading on the tensile properties of the BCP-filled rubber compounds before and after thermal aging. As shown clearly in Figure 6, the tensile strength of the composites increased with the addition of BCP. With the better dispersion of BCP,[54] the excellent frame structure could support the stress transferred from the matrix and effectively improve the tensile strength of the composites. The strong interfacial filler–rubber interaction, as shown from the values of α_f in Figure 3 was the other important factor. These results were in agreement with those of previous works.[55] As shown in Figure 7, the tensile modulus at 100 and 300% elongation increased with the addition of BCP. This indicated that the elasticity of the rubber chains was reduced with the addition of BCP. The increase in tensile modulus was associated with the M_H values of the composites; this increased with filler loading.[21]

As observed in Figure 8, the elongation at break increased until a maximum was obtained at 20 parts per hundred rubber (phr) and then decreased as the loading of BCP increased. This was due to the slippage of rubber chains from the surface of BCP. The improved elasticity may also have been due to the plasticizing effect of the gallery onium ions and the conformational effects on the polymer at the filler–matrix interface.[9] As the BCP loading increased, the elongation at break decreased gradually. Too much BCP led to aggregation; this brought more defects and formed the stress concentration point. The reduction in the elongation at break was mainly caused by the increasing stiffness and brittleness of the composite as a result

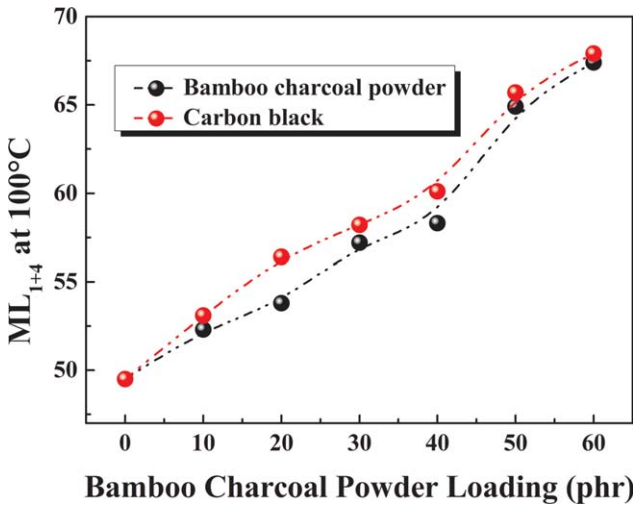

Figure 5. Mooney viscosity (ML_{1+4} at 100°C) values of the rubber compounds. [Color figure can be viewed in the online issue, which is available at wileyonlinelibrary.com.]

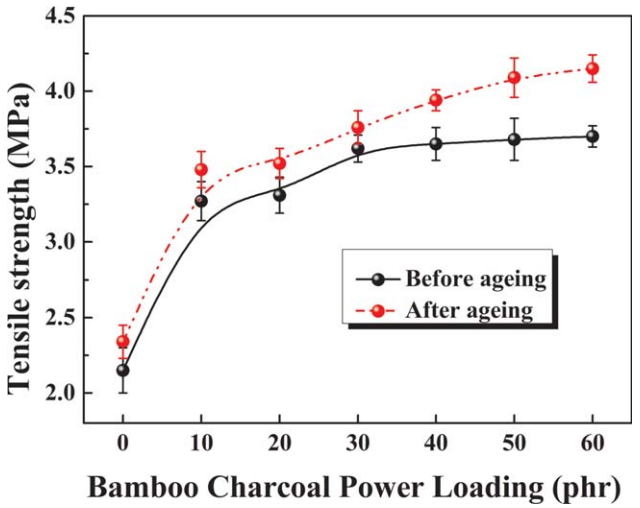

Figure 6. Effect of the BCP loading on the tensile strength of the rubber compounds. [Color figure can be viewed in the online issue, which is available at wileyonlinelibrary.com.]

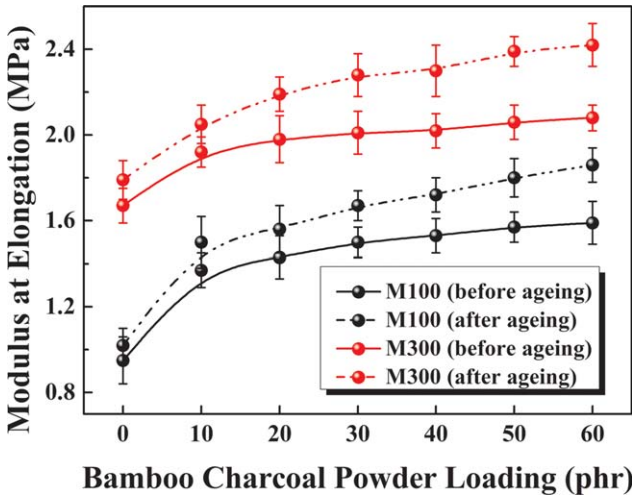

Figure 7. Effect of the BCP loading on the modulus at elongation values of the rubber compounds. [Color figure can be viewed in the online issue, which is available at wileyonlinelibrary.com.]

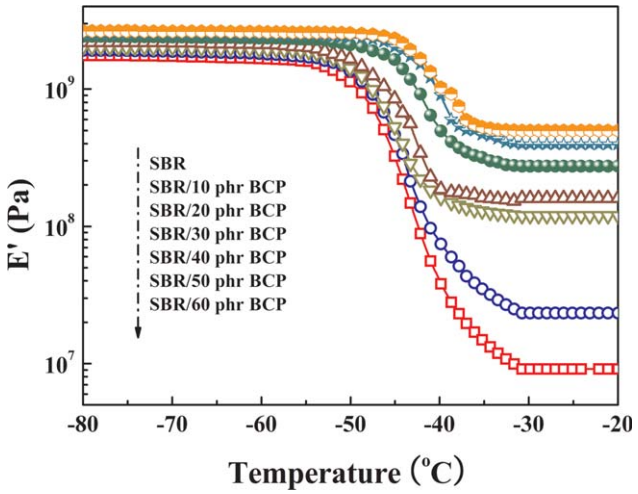

Figure 9. Effect of the BCP loading on the E' values of the rubber compounds. [Color figure can be viewed in the online issue, which is available at wileyonlinelibrary.com.]

of the transition from a rubber to a plastic phase with increasing BCP loading.[56] The increase in the filler loading tended to restrict the flexibility of the rubber chains and, therefore, caused the rubber vulcanizates to fail at a lower elongation.

The comparison of the mechanical properties of the BCP and carbon black is also shown in Table II. As shown, at a similar filler loading, the SBR materials filled with BCP had a lower tensile strength than that filled with carbon black. The macromolecular chains of rubber could mobilize in the original channels and porous structure, and the interfacial interaction of BCP–SBR, as shown from the values of α_f in Table II, was lower than that of carbon black. Compared to that filled with carbon black, the SBR filled with BCP had a better elongation at break because of the mobility of the macromolecular chains of rubber in the original channels and porous structure. The experimental results of thermal aging are also shown in Figures 6–8. It was interesting to note that after thermal aging, the tensile strength and modulus values at 100 and 300% elongation both increased gradually, whereas the elongation at break showed a decrease, which was due to the postcuring reaction.[57]

Dynamic Properties

DMA is a useful means for revealing the microscopic relaxation movement of polymer molecules. The results of DMA are described with the storage modulus (E') and tan δ in Figures 9 and 10, respectively, and the curves of E' versus the temperature for compounds with different BCP loadings are presented in Figure 9. As observed, E' increased with increasing BCP loading; this showed that the addition of BCP to the rubber resulted in an increase in stiffness. Furthermore, this indicated the strong confinement of BCP on the rubber chains. We also observed that E' dropped with increasing temperature; this indicated that all of the formulations gradually passed from stiff, hard, solid materials to soft and flexible materials.[58]

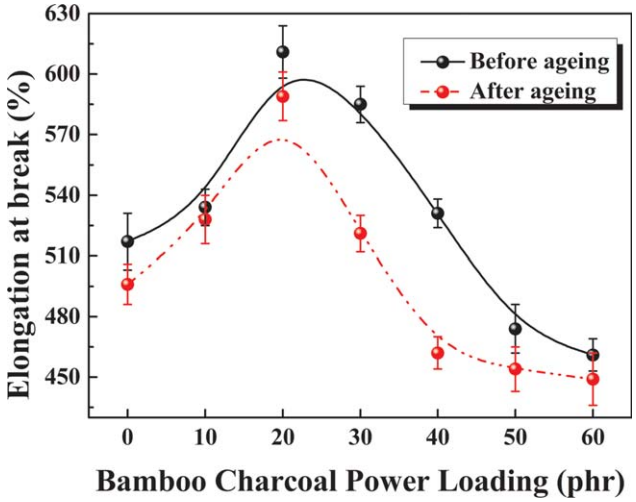

Figure 8. Effect of the BCP loading on the elongation at break of the rubber compounds. [Color figure can be viewed in the online issue, which is available at wileyonlinelibrary.com.]

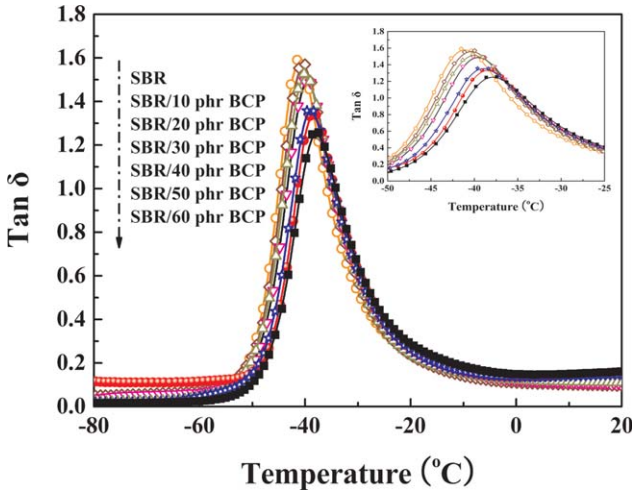

Figure 10. Effect of the BCP loading on the tan δ values of the rubber compounds. [Color figure can be viewed in the online issue, which is available at wileyonlinelibrary.com.]

Applied Polymer SCIENCE

Table III. Effects of the BCP Concentration on the T_g Values of the Rubber Composites

BCP content (phr)	T_g (°C)
0	−41.5
10	−40.8
20	−39.97
30	−39.4
40	−38.58
50	−37.95
60	−36.37

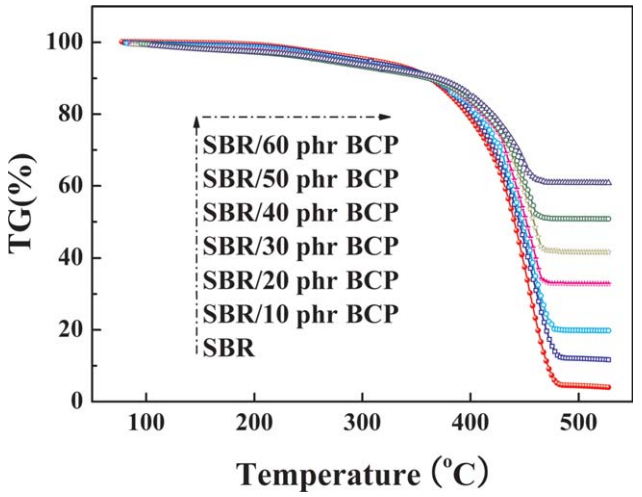

Figure 11. TG curves of the rubber compounds. [Color figure can be viewed in the online issue, which is available at wileyonlinelibrary.com.]

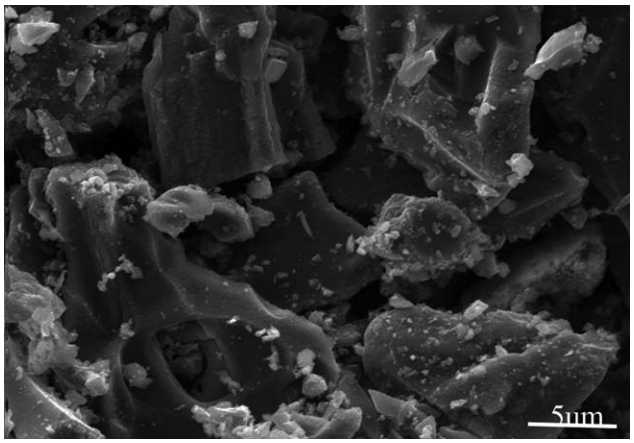

Figure 12. Surface morphology of the BCP.

The effect of BCP on the variation of tan δ as a function of the temperature is shown in Figure 10. According to the literature reported, the decrease in the α-transition peak height could have been related to the increase in the crosslinking density in the amorphous polymers.[59] As shown in Figure 10, the peak values of tan δ decreased with increasing BCP loading; this proved that the crosslinking density of the compounds increased and the crosslinking reaction played a more important role than the degradation. It is well known that the temperature at which tan δ shows a maximum is considered to be the T_g of the material. According to Figure 10, the T_g values of the compounds are shown in Table III. With increasing BCP loading, the T_g values of the compounds increased gradually. The new molecular interactions were formed at the boundaries; this resulted from the presence of BCP at the interface of the rubber.[6]

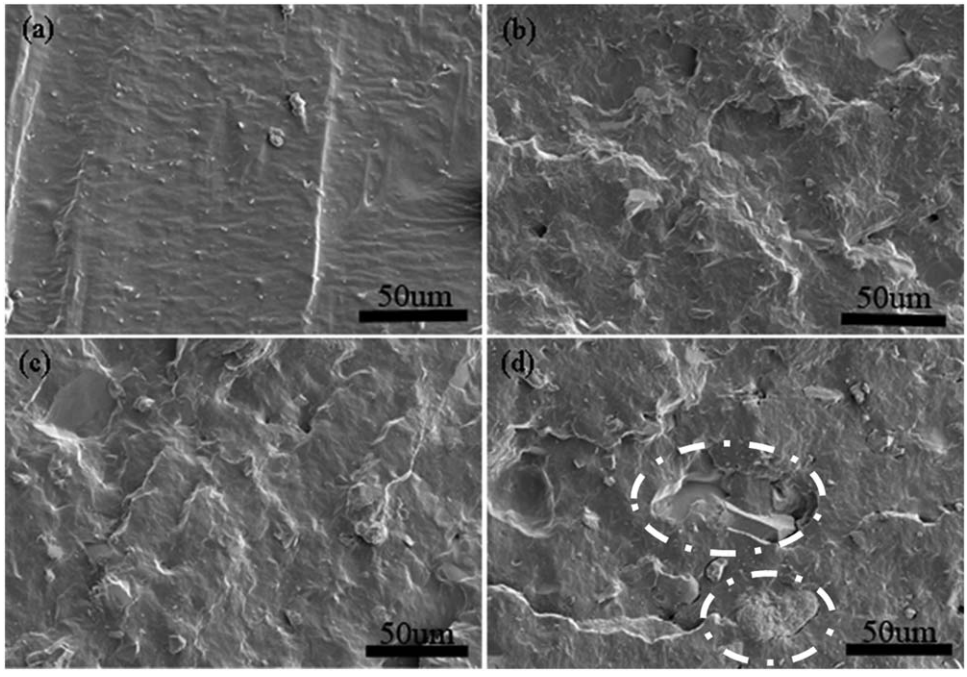

Figure 13. Fractured surface morphology of the SBR (a) without fillers and with (b) 10, (c) 20, and (d) 60 phr BCP.

Thermal Properties

The thermal stability of the compounds with different BCP loadings was studied by TG, and the TG curves are presented in Figure 11. As observed in Figure 11, as the BCP loading increased, the TG curves shifted right gradually; this indicated the thermal decomposition temperature increased gradually, and the thermal stability of the compounds improved. This may be have been because BCP, with its excellent thermal stability and low heat conduction coefficient, could efficiently restrict the heat transfer between the polymer chains and the thermal decomposition.

Morphological Studies of the Fractured Surface

The morphology of BCP is presented in Figure 12. As observed, BCP revealed the original channels and porous structure. This structure enabled better integration with the rubber chains and improved the properties of the compounds. The SEM micrographs in Figure 13 show the fractured surfaces of the compounds without BCP and with 10, 20, and 60 phr BCP taken at a magnification of 1000×. As shown in Figure 13(a), the fractured surfaces of SBR were smooth; however, the fractured surfaces of SBR filled with BCP were rough [Figure 13(b–d)]. We observed that BCP was dispersed uniformly in the rubber matrix, and the rubber was incorporated into the channels of BCP [Figure 13(b,c)]. The excellent dispersion and adhesion could have contributed to the improvement of the mechanical properties of the compounds, which were proven in a previous work. Figure 13(d) shows the SEM micrograph of SBR with 60 phr BCP. With increasing BCP loading, the dispersion of BCP in the rubber matrix became poor, and there were agglomerations and significant detachment of BCP from the rubber matrix. The formation of agglomeration and the significant detachment of BCP from the rubber matrix indicated that the resulting BCP detachment resulted in the reduction of the elongation at break.

CONCLUSIONS

The purpose of this study was to verify the possibility of using BCP as an alternative filler for SBR. t_{s2}, T_{90}, the torque (including M_H and M_L), the tensile strength, and the tensile modulus (M100 and M300, respectively) of the compounds increased with increasing BCP loading. E', T_g, and the decomposition temperature of the compounds increased, whereas the peak values of tan δ decreased with increasing BCP loading. Although, from the overall mechanical properties, BCP may have had a poorer reinforcing ability than that of carbon black, one may still consider the use of BCP as a filler in the rubber industry for economic and ecological reasons.

ACKNOWLEDGMENTS

This work was supported by the Fundamental Research Funds for the Central Universities (contract grant number 2652013063 and 2011PY0179), Key Project of Chinese Ministry of Education (contract grant number 107023), Special Fund of Co-Construction of Beijing Education Committee, City University of Hong Kong Strategic Research Grant (contract grant number 7008009), and the Doctoral Program Foundation of the Institution of Higher Education of China (contract grant number 2-2-08-07).

REFERENCES

1. Léon, D.; Sierra, P. L.; López, B. L. *Polym. Eng. Sci.* **2008**, *48*, 1986.
2. El-Nashar, D. E.; Ahmed, N. M.; Yehia, A. A. *Mater. Des.* **2012**, *34*, 137.
3. Wang, Q.; Zhang, Q.; Huang, Y.; Fu, Q.; Duan, X.; Wang, Y. *Chin. J. Polym. Sci.* **2008**, *26*, 495.
4. Da Costa, H. M.; Abrantes, T. A. S.; Nunes, R. C. R.; Visconte, L. L. Y.; Furtado, C. R. G. *Polym. Test.* **2003**, *22*, 769.
5. Prasertsri, S.; Rattanasom, N. *Polym. Test.* **2011**, *30*, 515.
6. Essawy, H.; El-Nashar, D. *Polym. Test.* **2004**, *23*, 803.
7. Liang, Y. R.; Wang, Y. Q.; Wu, Y. P.; Lu, Y. L.; Zhang, H. F.; Zhang, L. Q. *Polym. Test.* **2005**,*24*, 12.
8. Chakraborty, S.; Kar, S.; Dasgupta, S.; Mukhopadhyay, R.; Bandyopadhyay, S.; Joshi, M.; Ameta, S. C. *Polym. Test.* **2010**, *29*, 181.
9. Chakraborty, S.; Kar, S.; Dasgupta, S.; Mukhopadhyay, R.; Bandyopadhyay, S.; Joshi, M.; Ameta, S. C. *Polym. Test.* **2010**, *29*, 679.
10. Ismail, H.; Nizam, J. M.; A. Khalil, H. P. S. *Polym. Test.* **2001**, *20*, 125.
11. Da Costa, H. M.; Visconte, L. L. Y.; Nunes, R. C. R.; Furtado, C. R. G. *J. Appl. Polym. Sci.* **2002**, *87*, 1194.
12. Da Costa, H. M.; Visconte, L. L. Y.; Nunes, R. C. R.; Furtado, C. R. G. *J. Appl. Polym. Sci.* **2003**, *87*, 1405.
13. Da Costa, H. M.; Visconte, L. L. Y.; Nunes, R. C. R.; Furtado, C. R. G. *J. Appl. Polym. Sci.* **2003**, *90*, 1519.
14. Jamil, M. S.; Ahmad, I.; Abdullah, I. *J. Polym. Res.* **2006**, *13*, 315.
15. Khalf, A. I.; Ward, A. A. *Mater. Des.* **2010**, *31*, 2414.
16. Nakason, C.; Kaesman, A.; Homsin, S.; Kiatkamjornwong, S. *J. Appl. Polym. Sci.* **2001**, *81*, 2803.
17. Angellier, H.; Molina-Boisseau, S.; Dufresne, A. *Macromolecules* **2005**, *38*, 9161.
18. Liu, C.; Shao, Y.; Jia, D. M. *Polymer* **2008**, *49*, 2176.
19. Mélé, P.; Angellier-Coussy, H.; Molina-Boisseau, S.; Dufresne, A. *Biomacromolecules* **2011**, *12*, 1487.
20. Peterson, S. C. *J. Elastomers Plast.* **2012**, *44*, 43.
21. Ismail, H.; Shaari, S. M.; Othman, N. *Polym. Test.* **2011**, *30*, 784.
22. Ismail, H.; Rosnah, N.; Rozman, H. D. *Polymer* **1997**, *38*, 4059.
23. Ismail, H.; Jaffri, R. M. *Polym. Test.* **1999**, *18*, 381.
24. Jacob, M.; Thomas, S.; Varughese, K. T. *Compos. Sci. Technol.* **2004**, *64*, 955.
25. Nair, K. G.; Dufresne, A. *Biomacromolecules* **2003**, *4*, 657.
26. Nair, K. G.; Dufresne, A. *Biomacromolecules* **2003**, *4*, 666.
27. Nair, K. G.; Dufresne, A.; Gandini, A.; Belgacem, M. N. *Biomacromolecules* **2003**, *4*, 1835.
28. Poompradub, S.; Ikeda, Y.; Kokubo, Y.; Shiono, T. *Eur. Polym. J.* **2008**, *44*, 4157.
29. Wang, X. J.; Wang, Y.; Wang, X.; Liu, M.; Xia, S. Q.; Yin, D. Q.; Zhang, Y. L.; Zhao, J. F. *Chem. Eng. J.* **2011**, *174*, 326.

30. Zhao, R. S.; Wang, X.; Wang, X.; Lin, J. M.; Yuan, J. P.; Chen, L. Z. *Anal. Bioanal. Chem.* **2008**, *390*, 1671.
31. Mizuta, K.; Matsumoto, T.; Hatate, Y.; Nishihara, K.; Nakanishi, T. *Bioresour. Technol.* **2004**, *95*, 255.
32. Zhao, D. S.; Zhang, J.; Duan, E. H.; Wang, J. L. *Appl. Surf. Sci.* **2008**, *254*, 3242.
33. Zhang, J.; Zhao, D. S.; Wang, J. L.; Yang, L. Y. *J. Mater. Sci.* **2009**, *44*, 3112.
34. Zhu, J. T.; Huang, Z. H.; Kang, F. Y.; Fu, J. H.; Yue, Y. D. *New Carbon Mater.* **2008**, *23*, 326.
35. Ma, J. W.; Wang, H.; Wang, F. Y.; Huang, Z. H. *Sep. Sci. Technol.* **2010**, *45*, 2329.
36. Ma, J. W.; Wang, F. Y.; Huang, Z. H.; Wang, H. *J. Hazard. Mater.* **2010**, *176*, 715.
37. Wang, S. Y.; Tsai, M. H.; Lo, S. F.; Tsai, M. *J. Bioresour. Technol.* **2008**, *99*, 7027.
38. Lalhruaitluanga, H.; Jayaram, K.; Prasad, M. N. V.; Kumar; K. K. *J. Hazard. Mater.* **2010**, *175*, 311.
39. Wang, F. Y.; Wang, H.; Ma, J. W. *J. Hazard. Mater.* **2010**, *177*, 300.
40. Tan, Z. Q.; Qiu, J. R.; Zeng, H. C.; Liu, H.; Xiang, J. *Fuel* **2011**, *90*, 1471.
41. Asada, T.; Ohkubo, T.; Kawata, K.; Oikawa, K. *J. Health Sci.* **2006**, *52*, 585.
42. Hameed, B. H.; EI-Khaiary, M. I. *J. Hazard. Mater.* **2007**, *141*, 819.
43. Mui, E. L. K.; Cheung, W. H.; Valix, M.; McKay; G. *J. Hazard. Mater.* **2010**, *177*, 1001.
44. Ahmad, A. A.; Hameed, B. H. *J. Hazard. Mater.* **2010**, *175*, 298.
45. Wang, L. G.; Yan, G. B. *Desalination* **2011**, *274*, 81.
46. Mui, E. L. K.; Cheung, W. H.; Lee, V. K. C.; McKay; G. *Ind. Eng. Chem. Res.* **2008**, *47*, 5710.
47. Ten Brinke, J. W.; Debnath, S. C.; Reuvekamp, L. A. E. M.; Noordermeer, J. W. M. *Compos. Sci. Technol.* **2003**, *63*,1165.
48. Tan, J. H.; Wang, X. P.; Luo, Y. F.; Jia, D. M. *Mater. Des.* **2012**, *34*, 825.
49. Hassan, H. H.; Ateia, E.; Darwish, N. A.; Halim, S. F.; Abd El-Aziz; A. K. *Mater. Des.* **2012**, *34*, 533.
50. Siriwardena, S.; Ismail, H.; Ishiaku, U. S. *Polym. Test.* **2001**, *20*, 105.
51. Ismail, H.; Shaari, S. M. *Polym. Test.* **2010**, *29*, 872.
52. Ismail, H.; Rusli, A.; Rashid, A. A. *Polym. Test.* **2005**, *24*, 856.
53. Arayapranee, W.; Na-Ranong, N.; Rempel, G. L. *J. Appl. Polym. Sci.* **2005**, *98*, 34.
54. Myers, G. E.; Chahyadi, I. S.; Gonzalez, C.; Coberly, C. A.; Ermer, D. S. *Int. J. Polym. Mater.* **1991**, *15*, 171.
55. El-Nashar, D. E.; Mansour, S. H.; Girgis, E. *J. Mater. Sci.* **2006**, *41*, 5359.
56. Rao, V.; Johns, J. *J. Appl. Polym. Sci.* **2008**, *107*, 2217.
57. Sombatsompop, N.; Wimolmala, E.; Markpin, T. *J. Appl. Polym. Sci.* **2007**, *104*, 3396.
58. Garima, T.; Deepak, S. Mater. Sci. Eng., *A* **2007**, *443*, 262.
59. Diao, S.; Jin, K. K.; Yang, Z. Z.; Lu, H. F.; Feng, S. Y.; Zhang, C. Q. *Mater. Chem. Phys.* **2011**, *129*, 202.